MOLECULAR AND CELLULAR BIOLOGY, Oct. 2000, p. 7773–7783 Vol. 20, No. 20
0270-7306/00/$04.00+0

Meiotic Telomere Distribution and Sertoli Cell Nuclear Architecture Are Altered in *Atm*- and *Atm-p53*-Deficient Mice

HARRY SCHERTHAN,[1] MARTIN JERRATSCH,[1] SONU DHAR,[2] Y. ALAN WANG,[3] STEPHEN P. GOFF,[2] AND TEJ K. PANDITA[2]*

University of Kaiserslautern, D-67653 Kaiserslautern, Germany[1]; Columbia University, New York, New York 10032[2]; and Harvard Medical School, Boston, Massachusetts[3]

Received 31 January 2000/Returned for modification 20 June 2000/Accepted 18 July 2000

The ataxia telangiectasia mutant (ATM) protein is an intrinsic part of the cell cycle machinery that surveys genomic integrity and responses to genotoxic insult. Individuals with ataxia telangiectasia as well as *Atm*$^{-/-}$ mice are predisposed to cancer and are infertile due to spermatogenesis disruption during first meiotic prophase. *Atm*$^{-/-}$ spermatocytes frequently display aberrant synapsis and clustered telomeres (bouquet topology). Here, we used telomere fluorescent in situ hybridization and immunofluorescence (IF) staining of SCP3 and testes-specific histone H1 (H1t) to spermatocytes of *Atm*- and *Atm-p53*-deficient mice and investigated whether gonadal atrophy in *Atm*-null mice is associated with stalling of telomere motility in meiotic prophase. SCP3-H1t IF revealed that most *Atm*$^{-/-}$ *p53*$^{-/-}$ spermatocytes degenerated during late zygotene, while a few progressed to pachytene and diplotene and some even beyond metaphase II, as indicated by the presence of a few round spermatids. In *Atm*$^{-/-}$ *p53*$^{-/-}$ meiosis, the frequency of spermatocytes I with bouquet topology was elevated 72-fold. Bouquet spermatocytes with clustered telomeres were generally void of H1t signals, while mid-late pachytene and diplotene *Atm*$^{-/-}$ *p53*$^{-/-}$ spermatocytes displayed expression of H1t and showed telomeres dispersed over the nuclear periphery. Thus, it appears that meiotic telomere movements occur independently of ATM signaling. *Atm* inactivation more likely leads to accumulation of spermatocytes I with bouquet topology by slowing progression through initial stages of first meiotic prophase and an ensuing arrest and demise of spermatocytes I. Sertoli cells (SECs), which contribute to faithful spermatogenesis, in the *Atm* mutants were found to frequently display numerous heterochromatin and telomere clusters—a nuclear topology which resembles that of immature SECs. However, *Atm*$^{-/-}$ SECs exhibited a mature vimentin and cytokeratin 8 intermediate filament expression signature. Upon IF with ATM antibodies, we observed ATM signals throughout the nuclei of human and mouse SECs, spermatocytes I, and haploid round spermatids. ATM but not H1t was absent from elongating spermatid nuclei. Thus, ATM appears to be removed from spermatid nuclei prior to the occurrence of DNA nicks which emanate as a consequence of nucleoprotamine formation.

Ataxia telangiectasia is a rare human recessive autosomal disorder with a pleiotropic phenotype, specifically including progressive neurological degeneration, telangiectasia, often associated with premature aging, reduced size, immunodeficiency, sensitivity to ionizing radiation, cancer predisposition, and infertility (13, 40, 81, 93). Mice mutated in the homologue of the *ATM* (ataxia telangiectasia mutated) gene (*Atm*) display similar pleiotropic defects (5, 27, 97). The ATM protein belongs to a growing family of phosphatidylinositol-3 kinase-related kinases and seems to play a role as an intrinsic part of the cell cycle machinery that surveys genomic integrity, cell cycle progression, and processing of DNA damage. It shows similarity to several yeast and mammalian proteins involved in meiotic recombination and cell cycle progression, namely, the products of *MEC1* in the budding yeast *Saccharomyces cerevisiae* and *rad3*$^{+}$ of the fission yeast *Schizosaccharomyces pombe* (9, 56) and the TOR proteins of yeasts and mammals (45, 75). Besides its role in the mitotic cell cycle and development (14, 53, 98), the ATM protein and its relative ATR (ATM and rad3 related) have been regarded as important components in the machinery monitoring progression of meiotic recombination, double-strand break repair, and homologue pairing (60, 69), which is in agreement with the location of Atm throughout meiotic chromatin (7, 28). Detection and signaling of DNA damage are possibly mediated through downstream targets of ATM like c-Abl, Chk1, Chk2, and Rad51 proteins (8, 17, 19, 26). Furthermore, MEC1, the yeast homologue of the ATM phosphatidylinositol-3 kinase, is known to exert checkpoint function in the mitotic and meiotic cell cycle, and its absence mediates a defect in synapsis (35, 56). MEC1 is required for phosphorylation of replication protein A (Rpa) as a response to radiation-induced DNA damage (15). Rpa has been shown to interact with Rad51 (36), which plays an important role in meiotic recombination (82, 83, 89) and localizes to meiotic recombination complexes (1, 89, 90). Consistent with a role for ATM in meiosis, individuals with ataxia telangiectasia display gonadal atrophy and spermatogenetic failure, a phenotype which is mirrored by *Atm*-deficient mice (5, 97).

Cell lines derived from ataxia telangiectasia patients are hypersensitive to ionizing radiation (53, 58, 88) and display a prominent chromatin defect at chromosome ends in the form of chromosome end-to-end associations or telomeric associations seen at metaphase (49, 63, 64). Telomere associations correlate with genomic instability and carcinogenicity (21, 64, 65). Telomeres contain both DNA and protein that concertedly stabilize the ends of eukaryotic DNA, thereby protecting chromosome ends from exonucleolytic attack, fusion, and degradation (for reviews, see references 11 and 99). In the mammalian interphase nucleus, telomeres appear to be attached to the filamentous nuclear matrix (55), while in budding yeast cells, telomeres are clustered in a few perinuclear chromatin

* Corresponding author. Mailing address: Center for Radiological Research, College of Physicians & Surgeons, Columbia University, VC11-213, 630 West 168th St., New York, NY 10032. Phone: (212) 305-3911. Fax: (212) 305-3229. E-mail: tkp1@columbia.edu.

domains (20). Because of the *ATM* homology to *Mec1/Tel1* of *S. cerevisiae* (34, 74), it has been suggested that mutations in *ATM* could lead to altered telomere metabolism. We have recently reported alterations in both basal and radiation-induced telomeric associations and in mean telomere length in isogenic cells with manipulated ATM, demonstrating a direct link between ATM function and telomere maintenance (84). Furthermore, it was shown that *ATM* disruption leads to a telomeric chromatin defect in that telomere repeats are predominantly enriched in the insoluble nuclear matrix fraction (65, 85). $Atm^{-/-}$ spermatocytes I also have their telomeric repeats enriched in the nuclear matrix fraction and display an altered distribution of chromosome ends in the meiotic prophase nucleus, i.e., numerous nuclei have telomeres accumulated at a limited sector of the nuclear envelope (65)—a nuclear topology which resembles a chromosomal bouquet, which is usually seen at the leptotene-zygotene transition during meiotic prophase of the mouse (79) and other species (22, 100). Bouquet formation appears to be a consistent motif of meiotic prophase of the vast majority if not all eukaryotic species (for a review, see reference 23) and is thought to instigate interactions along aligned and spatially accumulated chromosome end segments. In this way it may bring about prealignment and facilitate the sorting process of homologues prior to their synaptic pairing (22, 54, 72, 91).

Spermatogenesis in male $Atm^{-/-}$ mice is disrupted during earliest prophase I, leading to chromosome fragmentation and spermatocyte degeneration during zygotene (5, 97). Aberrant zygotene-equivalent spermatocytes I of *Atm*-deficient mice frequently display a nuclear architecture of bouquet cells (65), which poses the question whether *Atm* inactivation stalls meiotic telomere movements at the cluster site. Here, we investigate telomere distribution in spermatocytes I of *Atm-p53* double-knockout mice, which show a partial rescue of progression through the first meiotic prophase (6). In this double mutant we observed a dramatic increase in the frequency of spermatocytes I with bouquet topology and show that a small number of mid-late pachytene and diplotene spermatocytes, as identified by the expression of the testis-specific histone H1 (H1t) and the synaptonemal complex protein SCP3, have telomeres dispersed over the nuclear periphery. Furthermore, it is shown that *Atm* disruption causes an immature nuclear architecture and heterochromatin distribution in Sertoli cells (SECs), the supportive somatic cell lineage of the seminiferous epithelium; they were found to display strong immunofluorescence (IF) Atm signals in their chromatin. Atm was detected in the chromatin of human SECs, mouse and human spermatocytes I, and developing spermatids.

MATERIALS AND METHODS

Mice and tissues. For the present study, we used mice that are deficient for *Atm*, *p53*, and c-*Abl* and double null for *Atm* and *p53*. The mating pairs for *Atm* heterozygotes were obtained from Philip Leder, Harvard Medical School, Boston. $p53^{+/-}$ mating mice were obtained from Larry Donehower, Baylor College of Medicine, Houston, Tex. The genotyping of the $Atm^{+/-}$, $p53^{+/-}$, and $Atm^{+/-}$ $p53^{+/-}$ mice was done by the procedure described by Westphal et al. (94), and the genotyping of c-*Abl* null mice was done according to the protocol of Hardin et al. (39). The alleles are carried on mixed genetic background mice (129SvEv × Black Swiss). Animal colonies were maintained at the animal care facility of Columbia University College of Physicians and Surgeons, New York. Generally, mice of 42 days of age were sacrificed, and testes were resected for further processing or instant snap freezing in liquid N_2. Frozen testicles were kept at −70°C until further use. Control IF experiments were also carried out on human testis biopsy material (79) which had been stored in liquid nitrogen.

Chromosome preparations, cell suspensions, and tissue sections. To obtain structurally preserved nuclei for three-dimensional analysis, male mice were killed by cervical dislocation. Testes were removed, and structurally preserved suspension nuclei were prepared by cross-linking fixation with phosphate-buffered saline (PBS)-buffered formaldehyde (65) and using the following modifications. Testicular fragments were minced with scalpels in cold minimal essential medium containing protease inhibitor (Roche Biochemicals). This suspension was mixed in equal volumes with fixative (3.7% formaldehyde, 0.1 M sucrose [pH 7.2]) and placed on silane-coated glass slides (Menzel Gläser). After air drying and prior to IF staining, the resulting sucrose coating was removed by rinsing the preparations repeatedly in PBS.

FISH. For fluorescence in situ hybridization, a directly labeled $(TTAGGG)_3$ PNA probe was used to detect telomere repeats (telo-FISH). When telo-FISH was combined with IF, we first performed immunostaining and then subjected preparations to simultaneous denaturation in the presence of the telomere probe (79). To mark the centromere-kinetochore region in SECs, we designed a 42-mer oligonucleotide (MiS1; 5′-GTGTA TATCA TAGAG TTACA ATGAG AAACA TGGAA AA-3′), which is homologous to the minor satellite of *Mus musculus* (95) and localizes to the kinetochore region of mouse metaphase chromosomes (see inset in Fig. 7e and not shown). Localization of minor satellite DNA to kinetochore regions of all *M. musculus* chromosomes has been reported previously (95). Labeling, FISH, and detection of oligonucleotides were performed as described (78).

Antisera. A polyclonal rabbit anti-SCP3 antiserum was utilized to detect axial cores and complete synaptonemal complexes (SCs) (52). A rabbit antiserum against testis-specific histone H1 (H1t) was used as previously described (59). An anti-cytokeratin 8 monoclonal antibody (MAb; clone 35βH11; Dako) and a goat antivimentin antiserum (31) were used to stain for SEC-specific intermediate filaments (3).

Two Abs to ATM were commercially obtained. Affinity-purified rabbit antiserum Ab1 (NB100-104) raised against an ATM fragment containing amino acids 2138 to 2739 expressed in *Escherichia coli* (27) was obtained from Novus Biologicals. An affinity-purified MAb to ATM, which was raised against a glutathione *S*-transferase fusion protein corresponding to amino acids 2577 to 3056 (2C1), was obtained from GeneTex, and its specificity in immunocytology and Western blots has been demonstrated earlier (7, 18). We tested the specificity of the Abs in mouse and human testis suspensions and performed IF analysis with the 2C1 MAb (18), since it produced a dispersed granular staining in both mouse and human testis suspension nuclei. Ab1 (Novus) was found to produce the same pattern of labeling in spermatocyte nuclei of both species, but in the mouse it additionally created strong granular IF signals throughout the sex vesicle (unpublished observations).

Immunostaining. IF staining of the SC lateral element SCP3 protein was done as described previously (65) with some modifications. Briefly, sucrose-embedded cells were washed with PBS, extracted for 30 min with 0.5% Triton X-100–PBS, and incubated with rabbit anti-SCP3 polyclonal serum diluted 1:1,000 in PTBG (PBS with 0.1% Tween 20, 0.2% bovine serum albumin, and 0.1% gelatin) overnight at 4°C. Cells were washed three times for 5 min each with PTBG and incubated with a secondary fluorescein isothiocyanate (FITC)-conjugated sheep anti-rabbit immunoglobulin (Ig) antibody (Sigma; diluted 1:250 in PTBG). After three washes in PBS-Tween 20 for 3 min each, preparations were mounted in antifade solution (Vector Laboratories) containing DAPI (4′,6′-diamidino-2-phenylindole; Sigma) (0.1 μg/ml) as DNA counterstain. For subsequent in situ hybridization, preparations obtained by this procedure were fixed for 5 min in PBS–0.1% formaldehyde (acid free; Merck), rinsed in PBS–0.1% glycine to quench aldehyde groups, and subjected to FISH (see above).

Immunostaining with Abs to cytokeratin 8 (MAb 35βH11; Dako) and vimentin (31) was done as described above. Vimentin was detected with secondary tetramethyl rhodamine isocyanate (TRITC)-conjugated anti-goat Ig Abs (Sigma; diluted 1:500 in PBS-Tween), while cytokeratin 8 was detected using secondary anti-mouse Ig-FITC Abs (Jackson Labs). Cytokeratin and vimentin immunoreactivity was verified on cytospin preparations of HeLa cells (not shown), which express both intermediate filament markers (61). Abs to ATM (diluted 1:100 in PTBG) were reacted with testis preparations as described above. Primary Abs were incubated with a biotinylated secondary Ab (Sigma; diluted 1:500 in PTBG), which was then visualized with ExtrAvidin-FITC (Sigma; diluted 1:500 in PTBG). Both Abs produced labeling throughout nuclear chromatin of testis suspension cells. The specificity of this chromatin-like labeling was verified by the absence of nuclear signals in $Atm^{-/-}$ testes nuclei or in reactions without the primary Abs (not shown).

RESULTS

Here, we investigate whether the aberrant meiotic telomere distribution caused by the *Atm* mutation (65) is retained in advanced spermatocytes of *Atm p53* double-knockout mice. Unlike in the *Atm* single mutant, spermatogenesis in the double mutant proceeds beyond the leptotene-zygotene transition although fertility is not restored (6). For further comparison, we also monitored spermatogenesis in mice deficient for genes which act downstream of *Atm*, namely *p53* and c-*Abl* (8, 43, 80).

To determine and verify the impact of the mutations studied on spermatogenesis, progression of meiotic prophase was

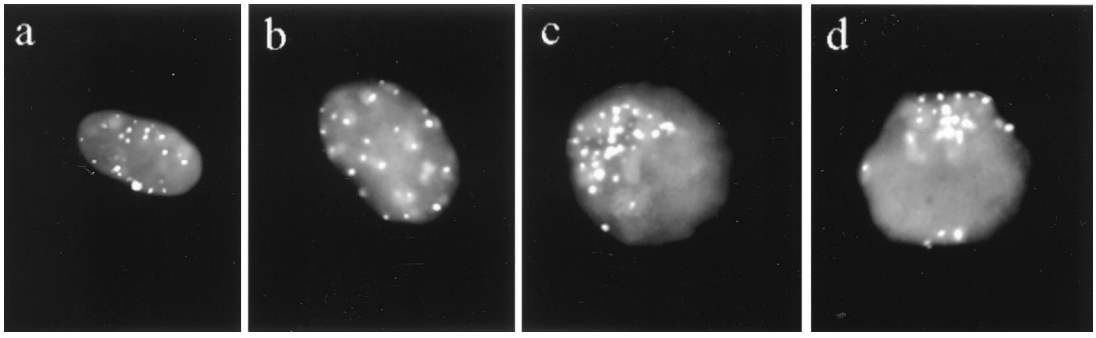

FIG. 1. PNA telo-FISH to testis suspension nuclei of *Atm-p53*-deficient mice. (a and b) Telomeres (whitish) are scattered throughout premeiotic, somatic nuclei (gray), as seen at the maximum nuclear diameter. (c and d) Top view of spermatocyte I nuclei which display telomeres clustered at a limited sector of the nuclear periphery (indicative of leptotene-zygotene transition). DNA was counterstained with DAPI (gray).

monitored by IF of SCP3 lateral element proteins (44, 76) of the SC in spread spermatocytes I of the various homozygous deletion mice (not shown) (65). In agreement with previous investigations (6, 7, 65, 97), our analysis revealed a meiotic prophase arrest in $Atm^{-/-}$ and $Atm^{-/-}$ $p53^{-/-}$ mice which manifested in a high frequency of aberrant spermatocytes showing defects in all aspects of SC formation, i.e., fragmented SCs, pairing-partner switches, absence of sex vesicle formation, and unpaired axial cores (not shown). Furthermore, we detected few late pachytene and diplotene cells as well as a few spermatids in $Atm^{-/-}$ $p53^{-/-}$ testis preparations (see below), which extends earlier observations according to which some $Atm^{-/-}$ $p53^{-/-}$ spermatocytes I reach the pachytene stage (6). Control, c-$Abl^{-/-}$ and $p53^{-/-}$ mice, in contrast, showed normal progression through male meiotic prophase (not shown). The fairly normal progression of early prophase I observed in the c-$Abl^{-/-}$ mice used in this investigation would be consistent with a role of c-*Abl* signaling in haploid spermatids (26, 70) and a variable phenotype according to which the majority of but not all c-$Abl^{-/-}$ mice exhibit defects in gametogenesis (50, 92). It is not known at present whether the action of the c-*Abl*-related tyrosine kinase Arg (50) is responsible for the variations in fertility in our c-*Abl* knockout mice.

$Atm^{-/-}$ $p53^{-/-}$ disruption causes a pronounced accumulation of spermatocytes with clustered telomeres. *Atm* disruption has been shown to increase the level of spermatocyte nuclei with locally clustered telomeres (bouquet arrangement) (65). To investigate whether this feature is also present in $Atm^{-/-}$ $p53^{-/-}$ spermatocytes I, we prepared testicular suspensions by cross-linking fixation with formaldehyde, which maintains nuclear topology to a considerable degree (65), and hybridized these in situ with a telomere repeat PNA probe (Fig. 1). When we assessed the frequency of nuclei with clustered telomeres in $Atm^{-/-}$ spermatocytes, a 32-fold increase over wild-type frequencies (0.12%) was noted (Table 1). Investigation of nuclear suspensions of $Atm^{-/-}$ $p53^{-/-}$ testicles revealed a further twofold increase in the frequency of spermatocytes with a bouquet topology compared to frequencies of $Atm^{-/-}$ testes, or, in other words, a 72-fold increase in bouquet cells over the control (Table 1).

Telomere clustering is relaxed in $Atm^{-/-}$ $p53^{-/-}$ mid-late pachytene spermatocytes. To address the question whether accumulation of bouquet spermatocytes results from immobilization of leptotene-zygotene telomeres, which are aberrantly associated with the nuclear matrix (65, 85), or whether the former effect is simply the consequence of prophase I arrest during zygotene, we assessed the topology of telomere distribution in $Atm^{-/-}$ and $Atm^{-/-}$ $p53^{-/-}$ spermatocytes. Advanced spermatocytes I can be identified by IF staining of testis-specific H1t and SCP3. H1t appears in mid-pachynema and is present until haploid spermatids reach the elongation stage (25, 59). Consistent with previous observations (59), H1t and SCP3 costaining revealed H1t fluorescence in the chromatin of undisrupted spermatocytes post-mid-pachytene and during diplotene as well as in round and elongated spermatids of wild-type mice (not shown). In $Atm^{-/-}$ testis suspensions, however, only one of several hundred spermatocytes investigated showed distinct H1t immunofluorescence and displayed characteristics of mid-pachytene SC formation, with strong labeling of partially polarized SCs having thickened ends (Fig. 2). Diplotene spermatocytes and haploid spermatids were absent in $Atm^{-/-}$ testis suspensions, which corroborates earlier findings showing that the vast majority of spermatocytes I get eliminated at the leptotene-zygotene transition (5, 7, 97).

H1t and SCP3 IF costaining of $Atm^{-/-}$ $p53^{-/-}$ testis suspensions disclosed the presence of mid-late pachytene spermatocytes (Fig. 3), which agrees with previous data (57, 59). In our mice we furthermore detected diplotene spermatocytes as well as round and elongated haploid spermatids (Fig. 3e and f and 4d to f). If stalling of meiotic telomere movements relates to *Atm* deficiency, one would expect H1t-positive late pachytene and diplotene $Atm^{-/-}$ $p53^{-/-}$ spermatocytes to be endowed with a bouquet topology. To test this possibility, we determined the mode of telomere distribution in *Atm-p53*-deficient spermatocytes by H1t IF and telo-FISH. Interestingly, it was found that chromosome ends were generally dispersed over the nuclear periphery of $Atm^{-/-}$ $p53^{-/-}$ post-mid-pachytene and diplotene spermatocytes (Fig. 4c to e). Thus, it appears that chromosome polarization is resolved during pachytene of $Atm^{-/-}$ $p53^{-/-}$ spermatocytes and that the

TABLE 1. Bouquet frequencies detected by telo-FISH in testis suspensions[a]

Cells	Bouquet frequency (%)	Bouquets (*n*)	Total no. of nuclei
Control	0.12	3	2,577
$p53^{-/-}$	0.16	4	2,505
$Atm^{-/-}$	3.9	31	788
$Atm^{-/-}$ $p53^{-/-}$	9.0	93	1,038

[a] Frequencies of nuclei with clustered telomeres were determined in testicular suspensions of different genotypes hybridized with a PNA telomere repeat probe. Nuclei with disrupted morphology, elongated spermatids, and sperm heads were excluded from the analysis.

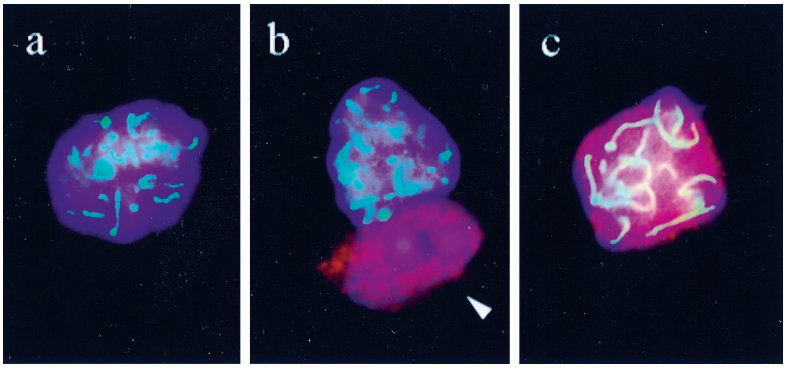

FIG. 2. Histone H1t (red) and anti-SCP3 (green) immunostaining to $Atm^{-/-}$ testis nuclei. (a) An aberrant spermatocyte I shows axial cores and fragments of SCs near a large chromocenter (bright blue). (b) Spermatocyte nucleus at zygotene equivalent stage with fragments of SCs is devoid of H1t signals. The SEC nucleus below (arrowhead) displays a large nucleolus (dark area void of H1t signal) and distinct dispersed H1t signals throughout its chromatin. Note that H1t signals were not seen in wild-type SECs (not shown). (c) A rare late-pachytene spermatocyte nucleus exhibiting H1t fluorescence and strongly labeled SCs with thickened ends. DNA is counterstained with DAPI (blue).

absence of functional ATM does not stall meiotic telomere movements.

***Atm*-deficient SECs express adult-type intermediate filament markers.** In the course of our H1t IF experiments, we repeatedly observed intense H1t signals in the chromatin of *Atm* mutant SECs (Fig. 3b), while an elevated H1t fluorescence in control SEC nuclei was generally absent (not shown). SECs of adult mammalian testes are mitotically inactive and represent the supporting cell lineage which is important for meiotic differentiation and maintenance of the blood-testis barrier (for reviews, see references 46 and 67). Since elevated H1t IF signals could suggest skewed or immature differentiation of *Atm*-deficient SECs, we examined the expression of vimentin and cytokeratin 8 in the mutants and control. Vimentin is an intermediate filament marker expressed by SECs throughout development (3, 24), while cytokeratin 8 expression marks lack of SEC differentiation, as it normally occurs only in fetal and early postnatal testes (2, 66) and in SECs of infertile individuals or in association with testicular cancer (10, 51, 61). IF disclosed an increased frequency of vimentin-positive mutant SECs in relation to total testis cells (Table 2), which is most likely related to the absence of haploid cells and/or a response to the requirements for increased phagocytosis of the apoptotic bodies resulting from massive germ cell degeneration in the knockouts. However, control, $Atm^{-/-}$, and $Atm^{-/-}$ $p53^{-/-}$ mutant SECs were found to exclusively express vimentin but not cytokeratin 8. A few cytokeratin 8-positive cells encountered in all genotypes (0.2% in the control and 0.3% in the mutants; not shown) most likely represent cells of the epididymis epithelium, which is known to express this intermediate filament (24). Therefore, it appears that *Atm* mutant SECs display a mature intermediate filament expression signature.

***Atm* localizes to the chromatin of SECs and spermatids.** Recently, ATM has been implicated in the control of histone H1 phosphorylation (36) and to be associated with histone

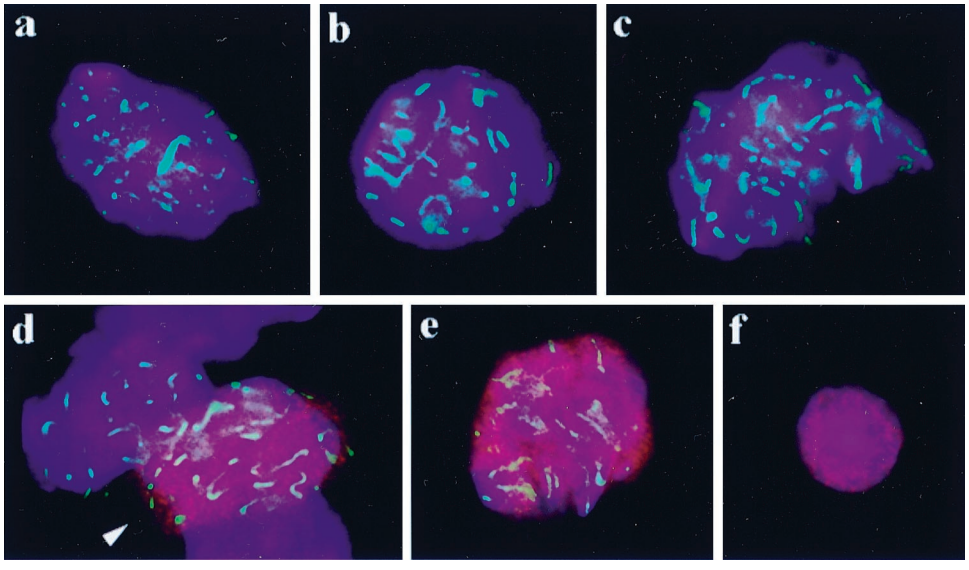

FIG. 3. H1t (red) and anti-SCP3 (green) immunostaining of $Atm^{-/-}$ $p53^{-/-}$ meiocytes. (a) Leptotene spermatocyte with faintly stained fragments of axial elements. (b) Zygotene nucleus with long axial elements and stronger SCP3 signal spots, which indicate some SC formation. (c) Aberrant spermatocyte I with fragmented SCs. Absence of H1t fluorescence indicates that this spermatocyte has not reached mid-pachytene. (d) Late-pachytene spermatocyte (arrowhead) with H1t-positive chromatin (red). (e) Diplotene spermatocyte with faintly labeled axial cores embedded in H1t-positive chromatin. (f) Nucleus of a round spermatid with a single DAPI-bright chromocenter and H1t-positive chromatin. DNA was stained with DAPI.

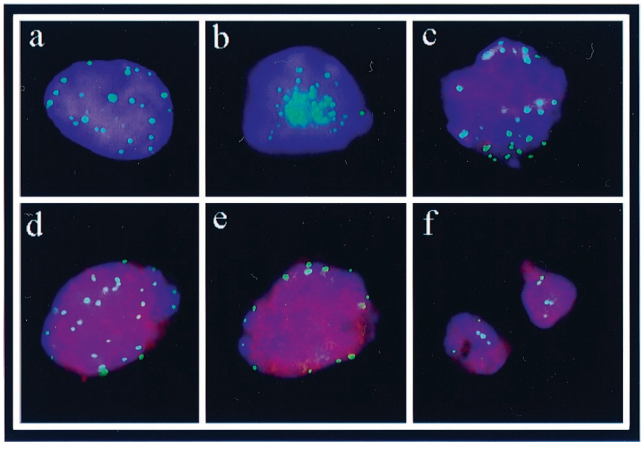

FIG. 4. Combined telo-FISH (FITC, green) and H1t immunostaining (Cy3, red) to suspension nuclei of $Atm^{-/-}$ $p53^{-/-}$ testis. (a) Premeiotic nucleus, which exhibits telomere signals (green) dispersed throughout the nuclear lumen, as seen at the focal plane at the nuclear center. (b) Top view of the nucleus of a bouquet spermatocyte discloses clustered telomeres at a limited sector of the nuclear periphery. This spermatocyte is most likely at leptotene-zygotene-equivalent stage, since H1t signals are absent. (c) A more advanced spermatocyte which displays faint H1t signals in its chromatin and a relaxed but still locally restricted accumulation of peripheral telomeres. Focal plane is at the top of nucleus. (d) H1t-positive spermatocyte nucleus (late pachytene or diplotene) exhibits dispersed telomeres. Focal plane is at top of nucleus. (e) The same nucleus as in panel d, but focal plane at the maximum nuclear diameter is shown. Telomeres are distributed over the nuclear periphery. (f) Two spermatid nuclei encountered in the $Atm^{-/-}$ $p53^{-/-}$ mouse testis show H1t fluorescence in their chromatin and formation of chromocenters. Nuclear DNA is counterstained with DAPI (blue).

deacetylase (47). Since the nature of the increased fluorescence of testis-specific histone H1t in *Atm*-deficient SECs remained unclear, we determined the presence of ATM in SECs by IF with MAb 2C1 (18). In the wild type, strong granular ATM IF signals were obtained throughout the nucleoplasm of SECs and other testis cell types (Fig. 5). A conspicuous dearth of ATM IF signal was noted at the heterochromatin blocks of SECs, while the euchromatic portion of the nuclei showed strong IF (Fig. 5c). In contrast, heterochromatin blocks of round spermatids in the same preparation showed the presence of H1t and, to a variable extent, of ATM epitopes at these regions (Fig. 5d), which indicates that the dearth of ATM signals in the heterochromatic chromocenters of SECs is not due to restricted access of Abs. Dispersed granular ATM signals were also noted throughout the nuclei of spermatocytes I and round spermatids. In the more advance spermatids, ATM fluorescence was less intense at the heterochromatin regions, while nuclei of elongated spermatids showed weak or no ATM signals at all. H1t-ATM costaining revealed that ATM was absent from nuclei of elongating spermatids which still displayed H1t epitopes (Fig. 5d). Sperm heads completely lacked ATM and H1t epitopes. These results are consistent with the replacement of histones and other chromatin and nucleoplasmic components by protamines during sperm maturation (4). Control IF experiments to testis suspensions of *Atm*-deficient animals revealed that ATM signals were generally absent from spermatogenetic and other cell types (Fig. 5). Occasionally, weak autofluorescence was observed in some preparations of $Atm^{-/-}$ testicles.

The fact that most of the antibodies used in IF studies to mouse spermatocytes were raised against portions of the human ATM protein (7) prompted us to test the specificity of our ATM MAb on human testis preparations. Reminiscent of the IF signals seen in the mouse, dispersed granular ATM epitopes were detected throughout the nuclei of all cell types of a human testis suspension (not shown). Decoration of axial cores or SCs with ATM, as reported before in mouse spreads (68, 69), was not detected in our undisrupted mouse and human spermatocytes. Altogether, it appears that the ATM protein is abundant in the nucleoplasm of spermatocytes, in developing round spermatids, and in the euchromatin of SECs. Its absence may influence the response of these cells to genotoxic insult as well as to differentiation-induced double-strand breaks in meiotic DNA.

SEC nuclear architecture is altered in *Atm*-deficient background. We furthermore determined whether the absence of the Atm protein also influences nuclear architecture and telomere distribution in SECs. In adult testes, most SECs display a unique nuclear architecture in that they carry a large nucleolus which is associated with one to three prominent DAPI-bright heterochromatin clusters amidst a faintly stained euchromatin (Fig. 6a to c) (37, 38, 41). In contrast to the adult situation, most SEC nuclei of prepubertal mouse testes contain numerous heterochromatin clusters (16). Using vimentin IF as an SEC marker on DAPI-stained testis preparations, we found that 79% or more of $Atm^{-/-}$ and $Atm^{-/-}$ $p53^{-/-}$ SEC nuclei contained four or more heterochromatin clusters of various sizes (Fig. 6d), which represents a threefold increase over the control (Table 3) and data in the literature (37, 41). It appears that the chromocenter distribution in *Atm*-mutant SECs is reminiscent of that of immature SECs (16). In addition to SECs with multiple heterochromatin clusters, both mutants contained a reduced number of SECs with two heterochromatin clusters, which are the predominant SEC type in the adult mouse (Table 3) (37, 38).

SECs of the adult mouse with one to three chromocenters have been shown to be present in two states: type I SECs have kinetochore dispersed over the corresponding chromocenters, while type II SECs have kinetochores tightly associated and are active in ribosomal gene transcription (38). To determine whether the Atm mutation influences the activity of SECs, we identified SEC types by marking mouse centromeres by FISH with a probe for the kinetochore-associated minor-satellite DNA of *M. musculus* (Fig. 6e, inset). Type I SECs, due to centromere dispersion over their corresponding chromocenter (38), did exhibit three or more minor-satellite signals per heterochromatin cluster (Fig. 6e). Type II SECs, due to tightly associated centromeres (38), displayed one or two strong minor satellite signals per heterochromatin cluster (Fig. 6f). Both *Atm* mutants were found to contain significantly more type I SECs than the control, in which type II SECs prevailed (Table 4). When we investigated associations of short-arm telomeres and centromeres in type II SECs by two-color FISH, it was found that heterochromatin blocks endowed with one or two minor-satellite FISH signals generally showed one or two strong telomere signals associated with a minor satellite cluster (Fig. 6f). Type I SECs generally exhibited telomere signals equaling the number of minor-satellite signals associated with

TABLE 2. Vimentin-positive SECs in mouse testis suspensions[a]

Cells	% Vimentin-positive SECs (no.)	No. of cells investigated
Control	7 (37)	531
$Atm^{-/-}$	23 (73)	319
$Atm^{-/-}$ $p53^{-/-}$	35 (186)	531

[a] Elongating spermatids and sperm heads were excluded from the evaluation to compensate for the lack of germ cells in the mutants.

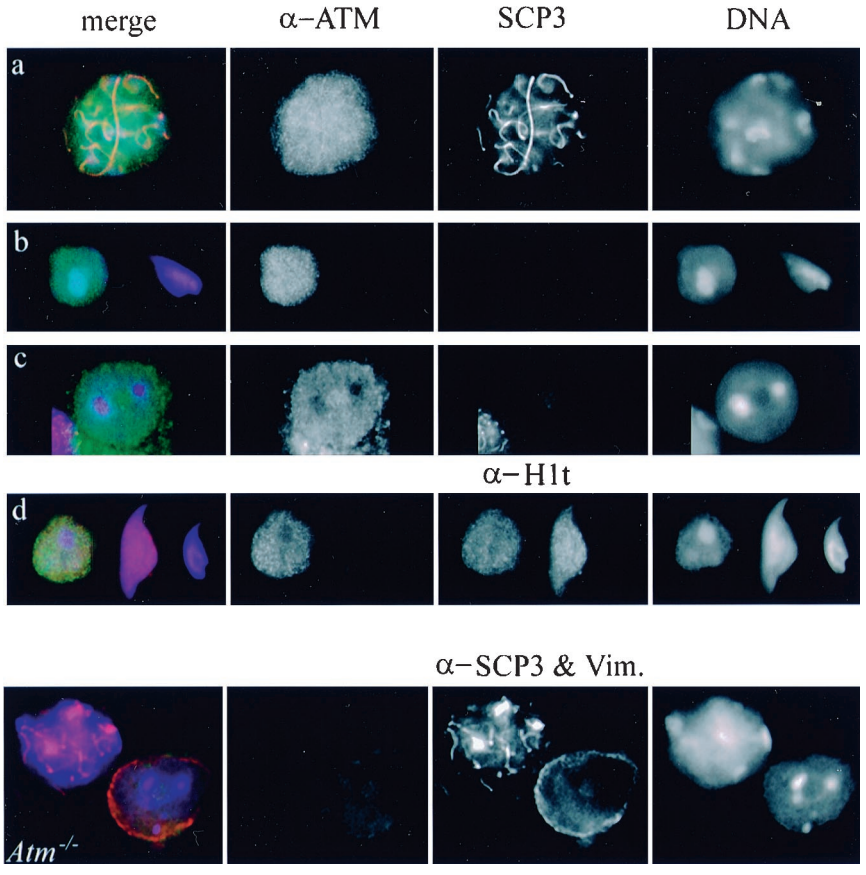

FIG. 5. IF staining of ATM (FITC, green) and SCP3 (red) in testis suspension cells of wild-type (a to c) and *Atm*$^{-/-}$ mice. Strong granular ATM IF signals are dispersed throughout the nuclei of (a) spermatocytes, (b) spermatids, and (c) SECs. Elongated sperm nuclei (c, right detail) do not exhibit ATM epitopes. ATM signals are reduced in the heterochromatin clusters of an SEC nucleus (c, dark-staining regions), while ATM is present in the heterochromatin clusters of a round spermatid (b). (d) ATM (green) and histone H1t (red) co-IF to wild-type spermatid nuclei. The round spermatid to the right shows extensive colocalization of ATM and H1t signals (yellow in the merge). The elongated spermatid nucleus in the center exhibits H1t but no ATM signals, while the condensed nucleus of a sperm head is void of IF signals. *Atm*$^{-/-}$, an *Atm*$^{-/-}$ spermatocyte (nucleus to the left, identified by SCP3-positive SC fragments [red]) and an SEC (as identified by vimentin [Vim.] staining around its nucleus; right detail in red channel) lack ATM immunofluorescence. The autofluorescence in the green channel seen at the SEC position results from weak bleedthrough of the strong vimentin signal upon prolonged exposure. DAPI was used as the DNA counterstain.

a chromocenter (Fig. 6e). These data indicate that telomere signal distribution in *Atm* mutant SECs is related to the activity status of SECs and that the absence of ATM does not induce defective telomere distribution in SECs. Therefore, it appears that type I SECs and those with immature nuclear architecture but adult intermediate filament expression profile are prevalent in the *Atm*-deficient background.

DISCUSSION

Individuals with ataxia telangiectasia and mice with *Atm* deficiency display gonadal atrophy and infertility. Previous investigation has revealed, in addition to other defects (for reviews, see references 13 and 53), that *Atm*$^{-/-}$ spermatocytes display altered telomere distribution. Here we show that the dramatic accumulation of spermatocyte I nuclei with a bouquet topology in *Atm*$^{-/-}$ mice (65) is also present in *Atm-p53* double-knockout mice. In this background, spermatogenesis proceeds beyond the leptotene-zygotene transition, although fertility is not restored (6). Immunostaining for SCP3 lateral element proteins and histone H1t showed the general absence of pachytene spermatocytes in *Atm*$^{-/-}$ testes, which confirms that spermatogenesis abrogates during zygotene equivalent stages (6, 65, 69, 97) in this background. In contrast to those from the single-knockout mice, testicles from our *Atm*$^{-/-}$ *p53*$^{-/-}$ mice were found to contain some pachytene and diplotene spermatocytes as well as a few round spermatids, which extends earlier reports that a subpopulation of *Atm*$^{-/-}$ *p53*$^{-/-}$ spermatocytes bypass the leptotene-zygotene arrest seen in the *Atm*$^{-/-}$ background (6).

***Atm*$^{-/-}$ *p53*$^{-/-}$ disruption causes pronounced accumulation of spermatocytes with clustered telomeres but fails to stall meiotic telomere movements.** ATM function has been shown to influence telomere metabolism in human systems (84), and telomere sequences are aberrantly associated with the nuclear matrix (85). Similar observations have been made in spermatocytes I of *Atm*$^{-/-}$ mice, which also display an elevated frequency of nuclei with a bouquet topology (65)—a nuclear organization motif which is rarely found in wild-type mouse spermatocytes (32, 79) and oocytes (87). The high frequency of bouquet cells encountered in the *Atm*$^{-/-}$ single-knockout mouse (65; this report) is further elevated in *Atm-p53* double-knockout mouse testes. The accumulation of prophase nuclei with bouquet topology in *Atm* mutant spermatogenesis indicates that most likely all mouse spermatocytes I pass through this under normal conditions. The accumulation of bouquet cells in the mutants could result from the absence of an Atm-dependent dispersion signal to clustered meiotic telomeres or,

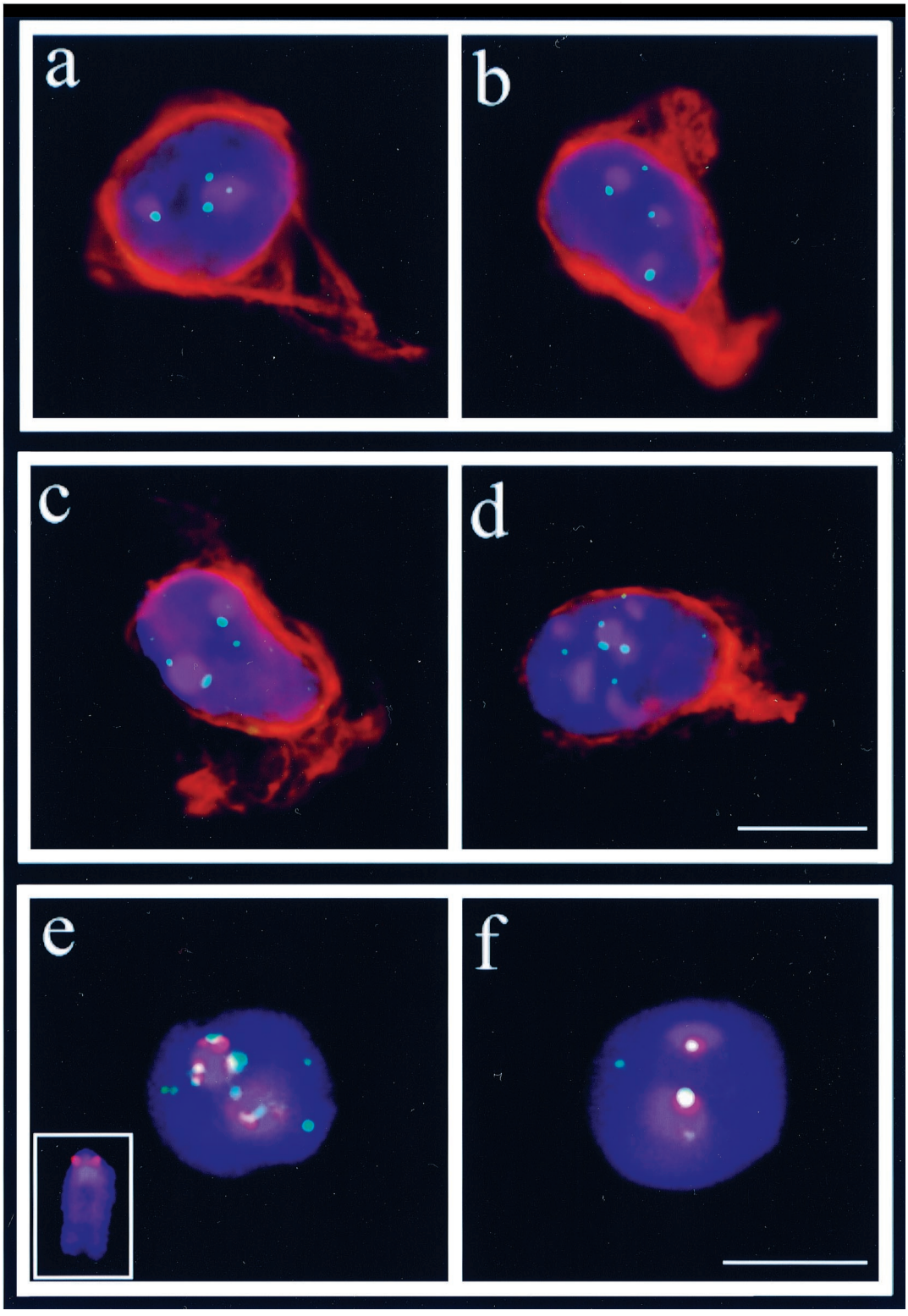

FIG. 6. SECs from control (a and b) and $Atm^{-/-}$ $p53^{-/-}$ mouse testis (c and d) stained for vimentin (TRITC; red) and hybridized with a FITC-labeled telomere PNA probe (fluorescein, green). (a to d) SECs positive for vimentin intermediate filament marker. (a) SEC with two chromocenters (blue) which are associated with one or two distinct telomere signals. (b) Vimentin-positive SEC with three chromocenters, each associated with one telomere signal. (c) Two-chromocenter *Atm* mutant SEC which shows two telomere signals at the larger chromocenter. (d) Mutant SEC with numerous heterochromatin clusters and telomere signals. The bar in d represents 10 μm and applies to a through d. (e) Wild-type two-chromocenter type I SEC with numerous minor-satellite (red) and associated telo-FISH signals (green). The inset shows an enlarged mouse metaphase chromosome (blue) with FISH signals of the minor-satellite probe (red) at the kinetochore region. (f) Nucleus of a wild-type two-chromocenter type II SEC which exhibits one strong minor-satellite signal (red) and an associated single-telomere signal (yellow) at each DAPI-bright chromocenter. DNA was counterstained with DAPI (blue). The bar in f represents 10 μm and applies to e and f.

TABLE 3. Heterochromatin cluster distribution in SEC nuclei

SECs (no.)	% with indicated no. of heterochromatin clusters		
	1	2	≥3
Control (129)	22	52	26
Atm$^{-/-}$ (209)	1	20	79
Atm$^{-/-}$ *p53*$^{-/-}$ (214)	0.5	12	87.5

[a] SECs were identified by vimentin immunostaining. In the wild type most nuclei displayed three clusters. Nuclei with up to eight clusters were occasionally seen. Nearly all *Atm* mutant nuclei contained more than 4 small clusters.

more likely, could simply be the consequence of accumulation of spermatocytes at the leptotene-zygotene transition, i.e., the stage when meiotic telomere clustering normally occurs (for reviews, see references 22, 77, and 100). The higher levels of bouquet cells observed in *Atm*$^{-/-}$ *p53*$^{-/-}$ mouse spermatogenesis and the presence of a few H1t-positive mid-late-pachytene and diplotene spermatocytes as well as a few round spermatids suggest that *Atm*$^{-/-}$ *p53*$^{-/-}$ mouse spermatocytes progress further in prophase I and more may reach the bouquet stage before they are doomed to apoptosis.

If zygotene telomeres are immobilized due to *Atm* deficiency, one would expect pachytene and diplotene spermatocytes to display a bouquet topology in the double mutant. Interestingly, we observed that chromosome ends were generally scattered over the nuclear envelope in the H1t-positive *Atm*$^{-/-}$ *p53*$^{-/-}$ late-pachytene nuclei investigated, which demonstrates that meiotic chromosome ends are capable of exerting positional changes in the absence of Atm signaling. The high frequency of bouquet cells detected in both *Atm* mutants therefore may be the consequence of slowed telomere movement to and at the cluster site. This could result from entrapment of chromosome ends by illegitimately connected chromosome cores, aberrant telomere-nuclear matrix interactions (65), and a generally slowed progression through leptotene-zygotene in *Atm*-deficient meiosis. Failure to establish faithful homologue pairing and to assemble recombination complexes (6, 7, 19, 97) may eventually trigger spermatocyte degeneration. In the double-knockout mice, the arrest is mediated in a p53-independent manner, which likely involves a synaptic checkpoint (62). If such a checkpoint operates in mammals, we would expect the few cells which reach and pass meiotic divisions to be derived from nuclei that were endowed with a premeiotic homologue association. In these cells, homologous synaptic pairing may have occurred without the detrimental effects which are elicited when separated homologous telomeres and chromosomes with distorted repair capacities are mobilized during a homologue search and tear apart chromosomes with double-strand breaks. According to this view, the degeneration of most *Atm-p53* double-knockout mouse spermatocytes would reflect the general absence of premeiotic homologue association in mammals (79).

SECs display an immature nuclear architecture in *Atm*-deficient genetic background. Since *Atm* function influences meiotic and mitotic telomere behavior and SECs usually display a few conspicuous telomere signals (telocenters) in tight association with their corresponding heterochromatin clusters (37, 79), we also determined whether short-arm telomere distribution of the acrocentric mouse chromosomes and nuclear architecture is affected by the *Atm* mutation. We used vimentin IF to identify SECs and found, in contrast to wild-type mice, that the majority of mutant vimentin-positive SECs contained numerous heterochromatin clusters, a nuclear architecture usually observed in SECs of immature postnatal testes (16). Without vimentin IF, such cells would have gone unnoticed. However, the adult intermediate expression profile suggests that SEC differentiation per se is not influenced by ATM function, since mutant SECs failed to express cytokeratin 8, a marker for immature or derailed SEC differentiation (2, 3). Besides SECs with immature heterochromatin distribution, the mutant testes also contained SECs with two heterochromatin clusters per nucleus, a feature frequently seen in normal adult mice. When we monitored the activity of the latter SECs with minor satellite and telo-FISH and applied the centromere criteria of Haaf et al. (38) (see Results), we found that most mutant SECs were of type I because they displayed centromeres and telomeres dispersed over the corresponding chromocenter. Furthermore, type I SECs have been shown to be inactive in ribosomal gene transcription (38). It has been suggested that the transcription of specific spermiogenesis genes at the onset of puberty and the initial formation of mature sperm coincide with maturation of nuclear architecture of SECs, i.e., the formation of one to three large heterochromatin clusters (16). This suggestion is supported by the immature nuclear topology and the inactive state of most mutant SECs with adult-type nuclear architecture in *Atm*$^{-/-}$ and *Atm*$^{-/-}$ *p53*$^{-/-}$ mouse testes, since both mutants fail to produce mature spermatozoa.

ATM localizes to the chromatin/nucleoplasm of SECs and haploid spermatids. Immunostaining of wild-type testes revealed granular overall fluorescence of ATM epitopes in the nucleoplasm of spermatocytes I, round spermatids, and SECs, which is consistent with a similar localization in somatic cells (30) and mouse spermatocytes (7). ATM IF signals were weak in elongating mouse spermatids which still displayed H1t epitopes, while both proteins were absent from sperm nuclei with a mature hook-shaped morphology. Our data indicate that ATM departs or is removed from spermatid chromatin prior to the stage when, in relation to the tight complexation of DNA with protamines, nicks (and possibly double-strand breaks) occur in sperm DNA (4, 86). ATM function in haploid cells will thus most likely contribute to surveillance of genome integrity prior to conversion of nucleosomal DNA into transcriptionally inert nucleoprotamine. In SECs, ATM was found at high levels throughout euchromatin, while prominent heterochromatin clusters of this cell type showed a dearth of ATM epitopes. This observation makes it unlikely that the lack of ATM at SEC heterochromatin directly influences chromocenter formation in this cell type. Reduced levels of ATM in heterochromatin of SECs (and maybe other cell types) could be linked to a reduced efficacy of DNA repair in inactive rodent chromatin (for a review, see reference 12). Exclusive colocalization of ATM with axial cores or SCs, as reported

TABLE 4. SEC types[a]

Cells	% of SECs		No. of nuclei analyzed
	Type I (≥3 minor-sat. signals)	Type II (1 or 2 minor-sat. signals)	
Control	31	69	61
Atm$^{-/-}$	71	29	52
Atm$^{-/-}$ *p53*$^{-/-}$	92	7	57

[a] SEC types were determined according to the number of minor-satellite (minor-sat.) DNA signals associated with a heterochromatin cluster. SECs endowed with one or two heterochromatin clusters were investigated for the presence of several minor-satellite centromere signals at the heterochromatin cluster were scored as type I, and those with one signal as type II (38).

previously from spread mouse spermatocytes (68, 69), was not observed in the undisrupted mouse and human spermatocyte nuclei in this study. Our data therefore align with recent IF studies in mouse meiosis, which showed a dispersed chromatin-like distribution in spermatocyte nuclei but failed to observe an exclusive preference of ATM for SC components (7, 60).

Overall, our findings argue against a prominent defect in telomere topology in *Atm* mutant spermatocytes I and SECs. The data can rather be reconciled with the view that the ATM protein kinase and its homologues are predominantly involved in mitotic and meiotic cell cycle control, possibly in response to DNA damage and double-strand break formation (35, 42, 56, 58, 96). The absence of ATM seems to slow progression of the initial stages of first meiotic prophase and, due to defective synapsis, also the formation and release of the bouquet topology, which results in the accumulation of spermatocytes with clustered telomeres, which are normally seen at the leptotene-zygotene transition stage (65, 79; this report). Interestingly, the *MEC1* mutant and other recombination-deficient mutants of *S. cerevisiae* display defects in synapsis (35, 48). Abrogated recombination has also been shown to lead to increased bouquet frequencies in yeast meiosis (91), which indicates a link between the two processes. Since spermatogenesis in *Atm*-deficient animals represents a pathological condition, further experiments are needed to disclose the players in the ATM-telomere act.

ACKNOWLEDGMENTS

We thank Raj Pandita for technical support, C. Heyting for SCP3 antiserum, P. Moens for H1t antiserum, and G. Giese for vimentin antiserum.

This work was supported by NIH grant NS34746 to T.K.P. and the Deutsche Forschungsgemeinschaft (350/8-2) to H.S.

REFERENCES

1. **Anderson, L. K., H. H. Offenberg, W. M. H. C. Verkuilen, and C. Heyting.** 1997. RecA-like proteins are components of early meiotic nodules in Lilly. Proc. Natl. Acad. Sci. USA **94:**6868–6873.
2. **Appert, A., V. Fridmacher, O. Locquet, and S. Magre.** 1998. Patterns of keratins 8, 18 and 19 during gonadal differentiation in the mouse: sex- and time-dependent expression of keratin 19. Differentiation **63:**273–284.
3. **Aumüller, G., C. Schulze, and C. Viebahn.** 1992. Intermediate filaments in Sertoli cells. Microsc. Res. Tech. **20:**50–72.
4. **Balhorn, R.** 1982. A model for the structure of chromatin in mammalian sperm. J. Cell Biol. **93:**298–305.
5. **Barlow, C., S. Hirotsune, R. Paylor, M. Liyanage, M. Eckhaus, F. Collins, Y. Shiloh, J. N. Crawley, T. Ried, D. Tagle, and A. Wynshaw-Boris.** 1996. Atm-deficient mice: a paradigm of ataxia telangiectasia. Cell **86:**159–171.
6. **Barlow, C., M. Liyanage, P. B. Moens, C. X. Deng, T. Ried, and A. Wynshaw-Boris.** 1997. Partial rescue of the prophase I defects of Atm-deficient mice by p53 and p21 null alleles. Nat. Genet. **17:**462–466.
7. **Barlow, C., M. Liyanage, P. B. Moens, M. Tarsounas, K. Nagashima, K. Brown, S. Rottinghaus, S. P. Jackson, D. Tagle, T. Ried, and A. Wynshaw-Boris.** 1998. Atm deficiency results in severe meiotic disruption as early as leptonema of prophase I. Development **125:**4007–4017.
8. **Baskaran, R., L. D. Wood, L. L. Whitaker, C. E. Canman, S. E. Morgan, Y. Xu, D. Baltimore, M. B. Kastan, and J. Wang.** 1997. Ataxia telangiectasia mutant protein activates c-Abl tyrosine kinase in response to ionizing radiation. Nature **387:**516–519.
9. **Bentley, N. J., D. A. Holtzman, G. Flaggs, K. S. Keegan, A. DeMaggio, J. C. Ford, M. Hoekstra, and A. M. Carr.** 1996. The *Schizosaccharomyces pombe* rad3 checkpoint gene. EMBO J. **15:**6641–6651.
10. **Bergmann, M., and S. Kliesch.** 1994. The distribution pattern of cytokeratin and vimentin immunoreactivity in testicular biopsies of infertile men. Anat. Embryol. (Berlin) **190:**515–520.
11. **Blackburn, E. H., and C. W. Greider (ed.).** 1995. Telomeres. Cold Spring Harbor monograph series no. 29. Cold Spring Harbor Laboratory, Cold Spring Harbor, N.Y.
12. **Bohr, V. A., and K. Wassermann.** 1988. DNA repair at the level of the gene. Trends Biochem. Sci. **13:**429–433.
13. **Bridges, B. A., and D. G. Harnden.** 1982. Ataxia telangiectasia: a cellular and molecular link between cancer, neuropathology, and immune deficiency. Wiley, Chichester, England.
14. **Brown, K. D., C. Barlow, and A. Wynshaw-Boris.** 1999. Multiple ATM-dependent pathways: an explanation for pleiotropy. Am. J. Hum. Genet. **64:**46–50.
15. **Brush, G. S., D. M. Morrow, P. Hieter, and T. J. Kelly.** 1996. The ATM homologue MEC1 is required for phosphorylation of replication protein A in yeast. Proc. Natl. Acad. Sci. USA **93:**15075–15080.
16. **Chandley, A. C., and R. M. Speed.** 1995. A reassessment of Y chromosome behaviour in germ cells and Sertoli cells of the mouse as revealed by in situ hybridisation. Chromosoma **104:**282–286.
17. **Chaturvedi, P., W. K. Eng, Y. Zhu, M. R. Mattern, R. Mishra, M. R. Hurle, X. Zhang, R. S. Annan, Q. Lu, L. F. Faucette, G. F. Scott, X. Li, S. A. Carr, R. K. Johnson, J. D. Winkler, and B. B. Zhou.** 1999. Mammalian Chk2 is a downstream effector of the ATM-dependent DNA damage checkpoint pathway. Oncogene **18:**4047–4054.
18. **Chen, G., and E. Y.-H. Lee.** 1996. The product of the *ATM* gene is a 370 kDa nuclear phosphoprotein. J. Biol. Chem. **271:**33693–33697.
19. **Chen, G., S. S. Yuan, W. Liu, Y. Xu, K. Trujillo, B. Song, F. Cong, S. P. Goff, Y. Wu, R. Arlinghaus, D. Baltimore, P. J. Gasser, M. S. Park, P. Sung, and E. Y.-H. Lee.** 1999. Radiation-induced assembly of Rad51 and Rad52 recombination complex requires ATM and c-*Abl*. J. Biol. Chem. **274:**12748–12752.
20. **Cockell, M., and S. M. Gasser.** 1999. Nuclear compartments and gene regulation. Curr. Opin. Genet. Dev. **9:**199–205.
21. **Counter, C. M., A. A. Avilion, C. E. LeFeuvre, N. G. Stewart, C. W. Greider, C. B. Harley, and S. Bacchetti.** 1992. Telomere shortening associated with chromosome instability is arrested in immortal cells which express telomerase activity. EMBO J. **11:**1921–1929.
22. **de Lange, T.** 1998. Ending up with the right partner. Nature **392:**753–754.
23. **Dernburg, A. F., J. W. Sedat, W. Z. Cande, and H. W. Bass.** 1995. The cytology of telomeres, p. 295–338. *In* E. H. Blackburn and C. W. Greider (ed.), Telomeres. Cold Spring Harbor monograph series no. 29. Cold Spring Harbor Laboratory, Cold Spring Harbor, N.Y.
24. **Dinges, H. P., K. Zatloukal, C. Schmid, S. Mair, and G. Wirnsberger.** 1991. Co-expression of cytokeratin and vimentin filaments in rete testis and epididymis: an immunohistochemical study. Virchows Arch. A Pathol. Anat. Histopathol. **418:**119–127.
25. **Drabent, B., C. Bode, B. Bramlage, and D. Doenecke.** 1996. Expression of the mouse testicular histone gene H1t during spermatogenesis. Histochem. Cell Biol. **106:**247–251.
26. **Duggal, R. N., Z. F. Zakeri, C. Ponzetto, and D. J. Wolgemuth.** 1987. Differential expression of the c-*Abl* proto-oncogene and the homeo box-containing gene Hox 1.4 during mouse spermatogenesis. Ann. N.Y. Acad. Sci. **513:**112–127.
27. **Elson, A., Y. Wang, C. J. Daugherty, C. C. Morton, F. Zhou, J. Campos-Torres, and P. Leder.** 1996. Pleiotropic defects in ataxia-telangiectasia protein-deficient mice. Proc. Natl. Acad. Sci. USA **93:**13084–13089.
28. **Flaggs, G., A. W. Plug, K. M. Dunks, K. E. Mundt, J. C. Ford, M. R. Quiggle, E. M. Taylor, C. H. Westphal, T. Ashley, M. F. Hoekstra, and A. M. Carr.** 1997. Atm-dependent interactions of a mammalian chk1 homolog with meiotic chromosomes. Curr. Biol. **7:**977–986.
29. **Gasior, S. L., A. K. Wong, Y. Kora, A. Shinohara, and D. K. Bishop.** 1998. Rad52 associates with RPA and functions with rad55 and rad57 to assemble meiotic recombination complexes. Genes Dev. **12:**2208–2221.
30. **Gately, D. P., J. C. Hittle, G. K. T. Chan, and T. J. Yen.** 1998. Characterization of ATM expression, localization, and associated DNA-dependent protein kinase activity. Mol. Biol. Cell **9:**2361–2374.
31. **Giese, G., M. Kubbies, and P. Traub.** 1990. Alterations of cell cycle kinetics and vimentin expression in asynchronous, TPA-treated MPC-11 mouse plasmacytoma cells. Exp. Cell Res. **190:**179–184.
32. **Glamann, J.** 1986. Crossing over in the male mouse as analyzed by recombination nodules and bars. Carlsberg Res. Commun. **51:**143–162.
33. **Golub, E. I., R. C. Gupta, T. Haaf, M. S. Wold, and C. M. Radding.** 1998. Interaction of human rad51 recombination protein with single-stranded DNA binding protein, RPA. Nucleic Acids Res. **26:**5388–5393.
34. **Greenwell, P. W., S. L. Kronmal, S. E. Porter, J. Gassenhuber, B. Obermaier, and T. D. Petes.** 1995. TEL1, a gene involved in controlling telomere length in *S. cerevisiae*, is homologous to the human ataxia telangiectasia gene. Cell **82:**823–829.
35. **Grushcow, J. M., T. M. Holzen, K. J. Park, T. Weinert, M. Lichten, and D. K. Bishop.** 1999. *Saccharomyces cerevisiae* checkpoint genes MEC1, RAD17 and RAD24 are required for normal meiotic recombination partner choice. Genetics **153:**607–620.
36. **Guo, C. Y., Y. Wang, D. L. Brautigan, and J. M. Larner.** 1999. Histone H1 dephosphorylation is mediated through a radiation-induced signal transduction pathway dependent on ATM. J. Biol. Chem. **274:**18715–18720.
37. **Guttenbach, M., M. J. Martinez-Exposito, W. Engel, and M. Schmid.** 1996. Interphase chromosome arrangement in Sertoli cells of adult mice. Biol. Reprod. **54:**980–986.
38. **Haaf, T., C. Steinlein, and M. Schmid.** 1990. Nucleolar transcriptional activity in mouse Sertoli cells is dependent on centromere arrangement. Exp. Cell Res. **191:**157–160.
39. **Hardin, J. D., S. Boast, P. L. Schwartzberg, G. Lee, F. W. Alt, A. M. Stall,**

and S. P. Goff. 1996. Abnormal peripheral lymphocyte function in c-abl mutant mice. Cell. Immunol. **172:**100–107.
40. **Harnden, D. G.** 1994. The nature of ataxia-telangiectasia: problems and perspectives. Int. J. Radiat. Biol. **66:**S13–S19.
41. **Hsu, T. C., J. E. Cooper, M. L. Mace, Jr., and B. R. Brinkley.** 1971. Arrangement of centromeres in mouse cells. Chromosoma **34:**73–87.
42. **Johnson, R. T., E. Gotoh, A. M. Mullinger, A. J. Ryan, Y. Shiloh, Y. Ziv, and S. Squires.** 1999. Targeting double-strand breaks to replicating DNA identifies a subpathway of DSB repair that is defective in ataxia-telangiectasia cells. Biochem. Biophys. Res. Commun. **261:**317–325.
43. **Kastan, M. B., Q. Zhan, W. S. El Deiry, F. Carrier, T. Jacks, W. V. Walsh, B. S. Plunkett, B. Vogelstein, and A. J. Fornace, Jr.** 1992. A mammalian cell cycle checkpoint pathway utilizing p53 and GADD45 is defective in ataxia-telangiectasia. Cell **71:**587–597.
44. **Keegan, K. S., D. A. Holtzman, A. W. Plug, E. R. Christenson, E. E. Brainerd, G. Flaggs, N. J. Bentley, E. M. Taylor, M. S. Meyn, S. B. Moss, A. M. Carr, T. Ashley, and M. E. Hoekstra.** 1996. The *Atr* and *Atm* protein kinases associate with different sites along meiotically pairing chromosomes. Genes Dev. **10:**2423–2437.
45. **Keith, C. T., and S. L. Schreiber.** 1995. PIK-related kinases: DNA repair, recombination, and cell cycle checkpoint. Science **270:**50–51.
46. **Kierszenbaum, A. L.** 1994. Mammalian spermatogenesis in vivo and in vitro: a partnership of spermatogenic and somatic cell lineages. Endocrine Rev. **15:**116–134.
47. **Kim, G. D., Y. H. Choi, A. Dimtchev, S. J. Jeong, A. Dritschilo, and M. Jung.** 1999. Sensing of ionizing radiation-induced DNA damage by ATM through interaction with histone deacetylase. J. Biol. Chem. **274:**31127–31130.
48. **Kleckner, N., R. Padmore, and D. K. Bishop.** 1991. Meiotic chromosome metabolism: one view. Cold Spring Harbor Symp. Quant. Biol. **56:**729–743.
49. **Kojis, T. L., R. A. Gatti, and R. S. Sparkes.** 1991. The cytogenetics of ataxia telangiectasia. Cancer Genet. Cytogenet. **56:**143–156.
50. **Kruh, G. D., R. Perego, T. Miki, and S. A. Aaronson.** 1990. The complete coding sequence of arg defines the Abelson subfamily of cytoplasmic tyrosine kinases. Proc. Natl. Acad. Sci. USA **87:**5802–5806.
51. **Kurohmaru, M., Y. Kanai, and Y. Hayashi.** 1992. A cytological and cytoskeletal comparison of Sertoli cells without germ cell and those with germ cells using the W/WV mutant mouse. Tissue Cell **24:**895–903.
52. **Lammers, J. H. M., H. H. Offenberg, M. van Aalderen, A. C. Vink, A. J. Dietrich, and C. Heyting.** 1994. The gene encoding a major component of the lateral elements of synaptonemal complexes of the rat is related to X-linked lymphocyte-regulated genes. Mol. Cell. Biol. **14:**1137–1146.
53. **Lavin, M. F., P. Concannon, and R. A. Gatti.** 1999. Eighth international workshop on ataxia-telangiectasia (ATW8). Cancer Res. **59:**3845–3849.
54. **Loidl, J.** 1990. The initiation of meiotic chromosome pairing: the cytological view. Genome **33:**759–778.
55. **Luderus, M. E. E., B. van Steensel, L. Chong, O. C. M. Sibon, F. F. M. Cremers, and T. de Lange.** 1996. Structure, subnuclear distribution, and nuclear matrix association of the mammalian telomeric complex. J. Cell Biol. **135:**867–881.
56. **Lydall, D., Y. Nikolsky, D. K. Bishop, and T. Weinert.** 1996. A meiotic recombination checkpoint controlled by mitotic checkpoint genes. Nature **383:**840–843.
57. **Meistrich, M. L., and W. A. Brock.** 1987. Proteins of the meiotic cell nucleus, p. 333–353. *In* P. B. Moens (ed.), Meiosis. Academic Press, New York, N.Y.
58. **Meyn, M. S.** 1995. Ataxia-telangiectasia and cellular responses to DNA damage. Cancer Res. **55:**5991–6001.
59. **Moens, P. B.** 1995. Histones H1 and H4 of surface-spread meiotic chromosomes. Chromosoma **104:**169–174.
60. **Moens, P. B., M. Tarsounas, T. Morita, T. Habu, S. T. Rottinghaus, R. Freire, S. P. Jackson, C. Barlow, and A. Wynshaw-Boris.** 1999. The association of ATR protein with mouse meiotic chromosome cores. Chromosoma **108:**95–102.
61. **Moll, R., W. W. Franke, D. L. Schiller, B. Geiger, and R. Krepler.** 1982. The catalog of human cytokeratins: patterns of expression in normal epithelia, tumors and cultured cells. Cell **31:**11–24.
62. **Odorisio, T., T. A. Rodriguez, E. P. Evans, A. R. Clarke, and P. S. Burgoyne.** 1998. The meiotic checkpoint monitoring synapsis eliminates spermatocytes via p53-independent apoptosis. Nat. Genet. **18:**257–261.
63. **Pandita, T. K., S. Pathak, and C. Geard.** 1995. Chromosome end association, telomeres and telomerase activity in ataxia telangiectasia cells. Cytogenet. Cell Genet. **71:**86–93.
64. **Pandita, T. K., E. J. Hall, T. K. Hei, M. A. Piatyszek, W. E. Wright, C. Q. Piao, R. K. Pandita, J. V. Willey, C. R. Geard, M. B. Kastan, and J. W. Shay.** 1996. Chromosome end-to-end associations and telomerase activity during cancer progression in human cells after treatment with a-particles simulating radon progeny. Oncogene **13:**1423–1430.
65. **Pandita, T. K., C. H. Westphal, M. Anger, S. G. Sawant, C. R. Geard, R. K. Pandita, and H. Scherthan.** 1999. Atm inactivation results in aberrant telomere clustering during meiotic prophase. Mol. Cell. Biol. **19:**5096–5105.
66. **Paranko, J., M. Kallajoki, L. J. Pelliniemi, V. P. Lehto, and I. Virtanen.** 1986. Transient coexpression of cytokeratin and vimentin in differentiating rat Sertoli cells. Dev. Biol. **117:**35–44.
67. **Parvinen, M., K. K. Vihko, and J. Toppari.** 1986. Cell interactions during the seminiferous epithelial cycle. Int. Rev. Cytol. **104:**115–151.
68. **Plug, A. W., A. H. Peters, Y. Xu, K. S. Keegan, M. F. Hoekstra, D. Baltimore, P. de Boer, and T. Ashley.** 1997. ATM and RPA in meiotic chromosome synapsis and recombination. Nat. Genet. **17:**457–461.
69. **Plug, A. W., A. H. Peters, K. S. Keegan, M. F. Hoekstra, P. de Boer, and T. Ashley.** 1998. Changes in protein composition of meiotic nodules during mammalian meiosis. J. Cell Sci. **111:**413–423.
70. **Ponzetto, C., and D. J. Wolgemuth.** 1985. Haploid expression of a unique c-*Abl* transcript in the mouse male germ line. Mol. Cell. Biol. **5:**1791–1794.
71. **Price, C. M.** 1999. Telomeres and telomerase: broad effects on cell growth. Curr. Opin. Genet. Dev. **9:**218–224.
72. **Rockmill, B., and G. S. Roeder.** 1998. Telomere-mediated chromosome pairing during meiosis in budding yeast. Genes Dev. **12:**2574–2586.
73. **Roeder, G. S.** 1997. Meiotic chromosomes: it takes two to tango. Genes Dev. **11:**2600–2621.
74. **Sanchez, Y., B. A. Desany, W. J. Jones, Q. Liu, B. Wang, and S. J. Elledge.** 1996. Regulation of RAD53 by the ATM-like kinases MEC1 and TEL1 in yeast cell cycle checkpoint pathways. Science **271:**357–360.
75. **Savitsky, K., A. Bar-Shira, S. Gilad, G. Rotman, Y. Ziv, L. Vanagaite, D. A. Tagle, S. Smith, T. Uziel, S. Sfez, M. Ashkenazi, I. Pecker, M. Frydman, R. Harnik, S. R. Patanjali, A. Simmons, G. A. Clines, A. Sartiel, R. A. Gatti, L. Chessa, O. Sanyal, M. F. Lavin, N. G. J. Jaspers, A. M. R. Taylor, C. F. Arlett, T. Miki, S. M. Weissman, M. Lovett, F. S. Collins, and Y. Shiloh.** 1995. A single ataxia telangiectasia gene with a product similar to PI-3 kinase. Science **268:**1749–1753.
76. **Schalk, J. A., A. J. Dietrich, A. C. Vink, H. H. Offenberg, M. van Aalderen, and C. Heyting.** 1998. Localization of SCP2 and SCP3 protein molecules within synaptonemal complexes of the rat. Chromosoma **107:**540–548.
77. **Scherthan, H.** 1997. Chromosome behavior in earliest meiotic prophase, p. 217–248. *In* H. Gill, J. S. Parker, and M. Puertas (ed.), Chromosomes today, vol. 12. Chapman and Hall, London, England.
78. **Scherthan, H., and T. Cremer.** 1994. Methodology of non isotopic in situ-hybridization in paraffin embedded tissue sections. Methods Mol. Genet. **5:**223–238.
79. **Scherthan, H., S. Weich, H. Schwegler, C. Heyting, M. Harle, and T. Cremer.** 1996. Centromere and telomere movement during early prophase of mouse and man are associated with the onset of chromosome pairing. J. Cell Biol. **134:**1109–1125.
80. **Shafman, T., K. K. Khanna, P. Kedar, K. Spring, S. Kozlov, T. Yen, K. Hobson, M. Gatei, N. Zhang, D. Watters, M. Egerton, Y. Shiloh, S. Kharbanda, D. Kufe, and M. F. Lavin.** 1997. Interactions between ATM protein and c-Abl in response to DNA damage. Nature **387:**520–523.
81. **Shiloh, Y.** 1995. Ataxia-telangiectasia: closer to unraveling the mystery. Eur. J. Hum. Genet. **3:**116–138.
82. **Shinohara, A., H. Ogawa, and T. Ogawa.** 1992. Rad51 protein involved in repair and recombination in *S. cerevisiae* is a RecA-like protein. Cell **69:**457–470.
83. **Shinohara, A., S. Gasior, T. Ogawa, N. Kleckner, and D. K. Bishop.** 1997. *Saccharomyces cerevisiae* recA homologues RAD51 and DMC1 have both distinct and overlapping roles in meiotic recombination. Genes Cells **2:**615–629.
84. **Smilenov, L. B., S. E. Morgan, W. Mellado, S. G. Sawant, M. B. Kastan, and T. K. Pandita.** 1997. Influence of ATM function on telomere metabolism. Oncogene **15:**2659–2665.
85. **Smilenov, L. B., S. Dhar, and T. K. Pandita.** 1999. Altered telomere nuclear matrix interactions and nucleosomal periodicity in ataxia telangiectasia cells before and after ionizing radiation treatment. Mol. Cell. Biol. **19:**6963–6971.
86. **Smith, A., and T. Haaf.** 1998. DNA nicks and increased sensitivity of DNA to fluorescence in situ end labeling during functional spermiogenesis. Biotechniques **25:**496–502.
87. **Speed, R. M.** 1982. Meiosis in the foetal mouse ovary. Chromosoma **85:**427–437.
88. **Suzuki, K., S. Kodama, and M. Watanabe.** 1999. Recruitment of ATM protein to double strand DNA irradiated with ionizing radiation. J. Biol. Chem. **274:**25571–25575.
89. **Tarsounas, M., T. Morita, R. E. Pearlman, and P. B. Moens.** 1999. RAD51 and DMC1 form mixed complexes associated with mouse meiotic chromosome cores and synaptonemal complexes. J. Cell Biol. **147:**207–220.
90. **Terasawa, M., A. Shinohara, Y. Hotta, H. Ogawa, and T. Ogawa.** 1995. Localization of RecA-like recombination proteins on chromosomes of the lily at various meiotic stages. Genes Dev. **9:**925–934.
91. **Trelles-Sticken, E., J. Loidl, and H. Scherthan.** 1999. Bouquet formation in budding yeast: Initiation of recombination is not required for meiotic telomere clustering. J. Cell Sci. **112:**651–658.
92. **Tybulewicz, V. L., C. E. Crawford, P. K. Jackson, R. T. Bronson, and R. C. Mulligan.** 1991. Neonatal lethality and lymphopenia in mice with a homozygous disruption of the c-abl proto-oncogene. Cell **65:**1153–1163.

93. **Westphal, C. H.** 1997. Cell-cycle signaling: Atm displays its many talents. Curr. Biol. **7:**789–792.
94. **Westphal, C. H., S. Rowan, C. Schmaltz, A. Elson, D. E. Fisher, and P. Leder.** 1997. Atm and p53 cooperate in apoptosis and suppression of tumorigenesis, but not in resistance to acute radiation toxicity. Nat. Genet. **16:** 397–401.
95. **Wong, A. K. C., and J. B. Rattner.** 1988. Sequence organization and cytological localization of the minor satellite of mouse. Nucleic Acids Res. **16:** 11645–11661.
96. **Xie, G., R. C. Habbersett, Y. Jia, S. R. Peterson, B. E. Lehnert, E. M. Bradbury, and J. A. D'Anna.** 1998. Requirements for p53 and the ATM gene product in the regulation of G1/S and S phase checkpoints. Oncogene **16:**721–736.
97. **Xu, Y., T. Ashley, E. E. Brainerd, R. T. Bronson, M. S. Meyn, and D. Baltimore.** 1996. Targeted disruption of ATM leads to growth retardation, chromosomal fragmentation during meiosis, immune defects, and thymic lymphoma. Genes Dev. **10:**2411–2422.
98. **Xu, Y., and D. Baltimore.** 1996. Dual roles of ATM in the cellular response to radiation and in cell growth control. Genes Dev. **10:**2401–2410.
99. **Zakian, V. A.** 1995. *Saccharomyces* telomeres: function, structure and replication, P. 107–138. *In* E. H. Blackburn and C. W. Greider (ed.), Telomeres. Cold Spring Harbor monograph series no. 29. Cold Spring Harbor Laboratory, Cold Spring Harbor, N.Y.
100. **Zickler, D., and N. Kleckner.** 1998. The leptotene-zygotene transition of meiosis. Annu. Rev. Genet. **32:**619–697.